

Band Notched UWB MIMO/Diversity Antenna Design with Inductance Boosted Compact EBG Structures

Naveen Jaglan^{1, *}, Priyanka Dalal², Samir D. Gupta¹, and Mahmoud A. Abdalla³

Abstract—A triple band notch MIMO/Diversity antenna using Inductance Boosted Compact Electromagnetic Band Gap (IB-CEBG) cells is presented in this paper. For obtaining compactness in the conventional EBG cell, spiral shaped defects are introduced. The proposed antenna obtains triple band notches in WiMAX (3.3–3.6 GHz), WLAN (5–6 GHz), and the X-band satellite communication (7.2–8.4 GHz) bands. IB-CEBG cells exhibits miniaturization of approximately 46% for WiMAX band, 50% for WLAN band and 48% for X-band Satellite communication band, compared to conventional EBG cells. To enhance the isolation among all four compact UWB monopoles, rectangular slots in the ground plane and parasitic decoupling arrangement are utilised. Further, a stepped structure with an angular separation of 90° is incorporated with individual monopoles to reduce mutual coupling effects. Stepped structure also helps in the better impedance matching by incrementing the path length. The results show that the magnitude of transmission coefficient is greater than 15 dB in between the ports of proposed antenna elements. Envelope Correlation Coefficient is less than 0.5, which lies in tolerable limits for Ultra-Wide band (UWB) frequency range. It has been noticed that notched frequency is dependent on IB-CEBG cell parameters. The proposed antenna is fabricated using an FR-4 substrate with overall dimensions of $58 \times 90 \times 1.6$ mm³.

1. INTRODUCTION

Ever since Federal Communications Commission unconstrained ultra-wide band (UWB) spectrum [1] for unrestricted commercial applications, there has been exponential growth in the design of UWB antennas. Simple UWB antenna designs like circular monopoles [2] are quite popular because of their several advantages like huge impedance bandwidth, easy fabrication, and excellent radiation performance. Some narrow band applications like WiMAX (3.3–3.6 GHz), WLAN (5–6 GHz), and X-Band satellite communication (7.2–8.4 GHz) bands interfere with UWB antenna. Therefore, to avoid such kind of interferences, band notched UWB antenna is needed. Several authors have worked and proposed various techniques that help in design of band notched antenna.

One such approach is reported in [3]. Here two dissimilar elliptic single complementary split-ring resonators (ESCSRRs) are etched over patch, and split-ring resonators are etched in joining antenna feed connection. This structure provides notches for different frequency bands, i.e., WiMAX, WLAN and X-band. A diamond-shaped patch multiband antenna (DSP) is reported in [4] that is integrated with several fine strips behaving as fine strips. In [5] with the help of Ω -type slot and resonant ring of semi octagon type in radiator and defected ground structure of hook shape on the ground plane, a triple band notched antenna is designed. In [6], the proposed antenna has triple band notch characteristics

Received 24 July 2020, Accepted 9 September 2020, Scheduled 22 September 2020

* Corresponding author: Naveen Jaglan (naveenjaglan1@gmail.com).

¹ Department of Electronics & Communication Engineering, Jaypee University of Information Technology, Waknaghat, Solan, Himachal Pradesh, India. ² Department of Electronics & Communication Engineering, Guru Jambheshwar University of Science & Technology, Hisar, Haryana, India. ³ Electromagnetic Waves Group, Electronic Engineering Department, MTC College, Kobery Elkobba, Cairo, Egypt.

using three open-ended quarter wavelength slots. The band rejections features can be attained by implementing the feed line [7] with the band reject elements of the UWB antenna. In [8], a conventional slot of quarter-wavelength with open ends is engraved in the radiator, and to obtain triple band notches, the radiating element has three half wavelength semicircular slots. Several other triple band notched antennas utilising similar techniques are proposed by in [9–12]. Electrical ring resonator [13] and hollow cross-loop resonators [14] are used to obtain triple band notches. The proposed antenna in [15] uses slots in the microstrip feed to obtain triple band notches. In [16] using fire-fly algorithm and particle swarm optimization, a triple band notch antenna is shown. Further, three notches can also be obtained by modifying radiator [17] with several slots. U-shaped type slots in ground and arc shaped slots [18] in the radiators are used to obtain notches in radiators to obtain triple band notches. Radiator and ground plane [19] etched with c-shaped slots obtain triple notches. Most of the techniques discussed are dependent on antenna shape and do not have proper control on notch width and location. If the approach antenna shape dependent, then one method methodology might not be suitable for another antenna structure. Some antenna shape independent approaches are also reported by several researchers. In [20, 21], the authors show that WLAN band notches can be obtained using EBG structures. In [20], one band notch is obtained by using four EBG structures around the antenna feed.

MIMO communication system demands multiple antenna elements at transmitter and receiver sides with reduced mutual coupling. MIMO antenna improves data rate and link reliability in multipath communication system. UWB MIMO systems also provide enhanced channel capacity compared with narrowband systems [22]. Several UWB MIMO antennas are proposed by different researchers in [23–25]. However, electromagnetic coupling in radiating elements degrades the performance [26, 27] of MIMO systems significantly. Various techniques are proposed to reduce mutual coupling in radiating elements like slotted ground plane [28–30], novel antenna designs [31, 32], EBG structures [33, 34], etc. Most of the designs [35–37] do not work over the complete UWB frequency range.

Extensive research has been performed in the investigation of the band-rejection features of the MIMO antennas [38–43]. In [44], open ended slots and parasitic strips are used to obtain band notch characteristics. In [45], two element G-shaped antenna designs with WLAN band notch are reported. Most of the MIMO systems obtain band notches by altering the radiator thereby affecting the radiation performance.

In the proposed structure, a MIMO network comprising four semi-circular stepped monopole structures with an angular separation of 90° is implemented for UWB application. To lessen the effect of mutual coupling, decoupling elements with slotted antenna ground is utilised. In this paper, circular traditional UWB antennas are modified in stepped case, and IB-CEBGs are used to have triple band notches at WiMAX, WLAN, and X-Band satellite communication bands. Technique utilised in obtaining band notches is independent of the antenna design and based on certain set of formulas. The effects of variation of different parameters of IB-CEBG structures on band notches are also explained.

2. CREATION OF THE DESIRED BAND GAP FOR CIRCULATING SURFACE WAVES USING EBG STRUCTURES

Mushroom EBG structures are a type of frequency selective surface. EBG structures have high impedance in certain frequency bands hence also known as high impedance structures [46–51] and can be used for obtaining band notches in UWB antennas. An EBG structure consists of a conducting patch that is connected to ground plane through metallic via. The electrical equivalent of EBG circuits forms a parallel LC circuit. Inductance L arises because current flows in conducting via, but capacitance C is due to spacing amid the EBG patches. The important design formulas relating L and C with the dimensions of EBG structures [46] are:

$$L = 0.2h \left[\ln \left(\frac{2h}{r} \right) - 0.75 \right] \quad (1)$$

$$C = \varepsilon_0 \varepsilon_r \frac{W^2}{h} \quad (2)$$

$$\omega_0 = \frac{1}{\sqrt{LC}} \quad (3)$$

Here W is the square EBG cell width, C the capacitance, L the inductance, ϵ_r the relative permittivity, ϵ_0 the absolute permittivity, h the via height, r the via radius, and ω_0 the resonant frequency. These equations will be served as basic equations for the proposed IB-CEBG structures.

3. STEPWISE DESIGN OF PROPOSED ANTENNA

Planar circular monopole is considered as the basic antenna element in this paper. This antenna element is modified by using stepped structures so as to have better impedance matching and reduced mutual coupling. Impedance matching is achieved because this stepped structure will have overall perimeter same as that of circular monopole. Mutual coupling is reduced because the spacing among the radiators is increased in stepped structures. IB-CEBG cells situated near antenna feed are responsible for notches at interfering bands.

The proposed IB-CEBG structures are a modified version of mushroom EBG structures having spiral shaped slots. This will boost the value of inductance and make these structures compact.

If only one band creates interference in UWB frequency range, then single notch is essential. Therefore, only a single pair of EBG structures is required. When the interference is from WiMAX, WLAN, and the X-band, then three different IB-CEBG cells of different dimensions are required. The bigger IB-CEBG cell is accountable for the rejection of WiMAX band frequencies, and the smallest one is responsible for the notch in X-band.

Figure 1 reveals the expansion of suggested structure using UWB MIMO/Diversity antenna by means of IB-CEBG cells.

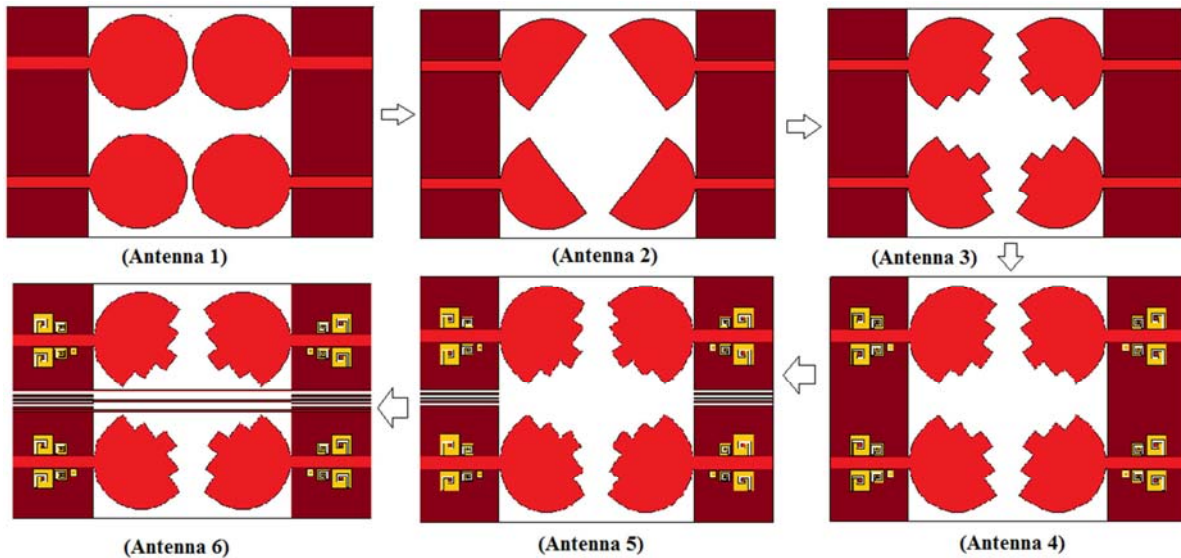


Figure 1. Step by step expansion of the proposed MIMO/Diversity antenna.

Antenna 3 have an enhanced perimeter as compared to antenna 2. The more the antenna perimeter is, the more the current path circulation length will be which helps in impedance matching [52] with the same microstrip feed. In antenna 4, IB-CEBG cells are used to obtain triple band notch characteristics.

$$f_r = \frac{1}{2\pi\sqrt{(L_1 + L_2 + L_3)(C_1 + C_0)}} \tag{4}$$

In antenna 5, slotted ground plane is used to minimise mutual coupling effect. In antenna 6, decoupling strips [53] are used on the top of the substrate to further minimise coupling effects. Decoupling strips along with slotted ground planes provide UWB isolation from 3.1 to 10.6 GHz. Different steps are shown and used to reach the proposed antenna 6 which has precise triple band notches at interfering

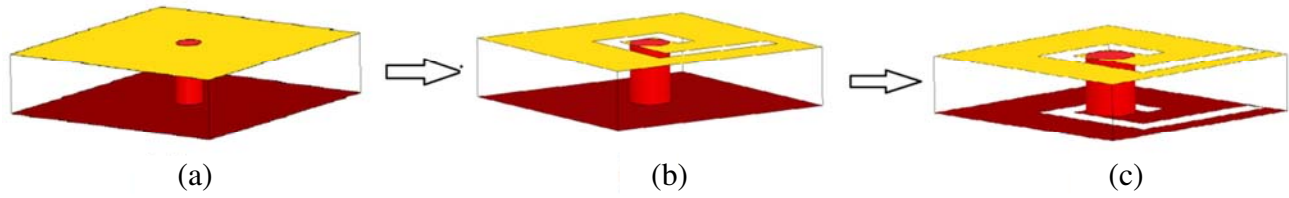


Figure 2. Evolution of IB-CEBG structure from the mushroom EBG structure.

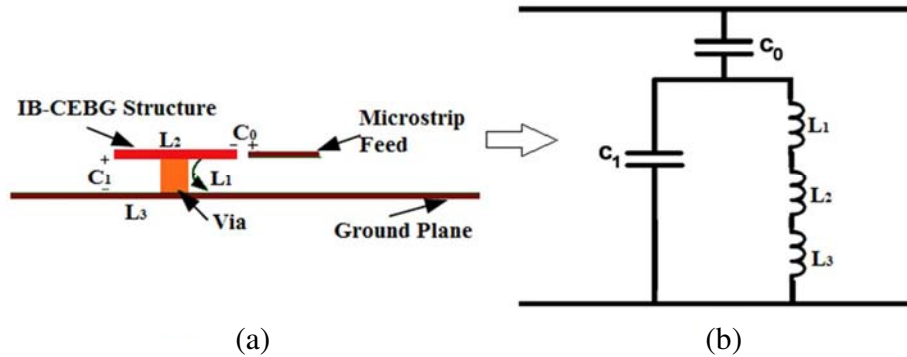


Figure 3. (a) IB-CEBG structure placed with microstrip line; (b) Equivalent circuit.

frequencies with minimized mutual coupling among antenna elements. Fig. 2 shows the steps taken to reach up to IB-CEBG structures. Two spiral shaped slots are etched on the top and bottom conducting patches of a conventional EBG structure. In Fig. 3, the electrical equivalent circuit of an IB-CEBG structure with microstrip feed is given. The resonant frequency for this circuit is given in Equation (4). L_2 and L_3 help in inductance boosting due to spiral shaped slots on the top and bottom surfaces of a conventional EBG structure.

4. RESULTS AND DISCUSSION

The proposed antenna design with IB-CEBG cells is shown in Fig. 4. Fig. 5 shows various steps that are used to reach up to proposed IB-CEBG structures. IB-CEBG structures for WiMAX and WLAN bands have the same number of turns. However, IB-CEBG for X-band has a large number of turns. Higher number of turns will boost inductance to a higher level, and thus single X-band IB-CEBG cell will give the same effect as given by the WiMAX and WLAN pairs. In Table 1, all design dimensions of proposed antenna are provided. Fig. 6 shows the surface current distribution on the proposed antenna structure. It can be seen that the maximum current is available on the IB-CEBG cells in their bandgaps, which does not allow much current to pass the radiator thereby generates notches. In Fig. 7, the fabricated antenna prototype is shown. A low cost FR-4 substrate with the relative permittivity of 4.4, loss tangent of 0.002, and thickness of 1.6 mm is used in the design. The simulation of proposed design is done using Ansoft HFSS v.17. The s -parameters measurement is done using AgilentTM Network Analyzer PNA-L series. A microwave shielded anechoic chamber is used for the measurement of antenna gain and radiation pattern. Fig. 8 shows the simulated values of VSWR for the proposed antenna along with all intermediate antennas. It can be seen that the proposed antenna has triple notches ($VSWR > 2$) in three interfering bands which are WiMAX, WLAN, and X-band satellite communication bands. At these frequencies, the input power will not reach the radiator and concentrates on the respective IB-CEBG structures. The perimeters of radiators in antenna 1 and antenna 3 are the same giving similar variations of VSWR. The focus of antenna 4 and antenna 5 is on the minimisation of mutual electromagnetic coupling without affecting the initially attained notches. This is the reason that the

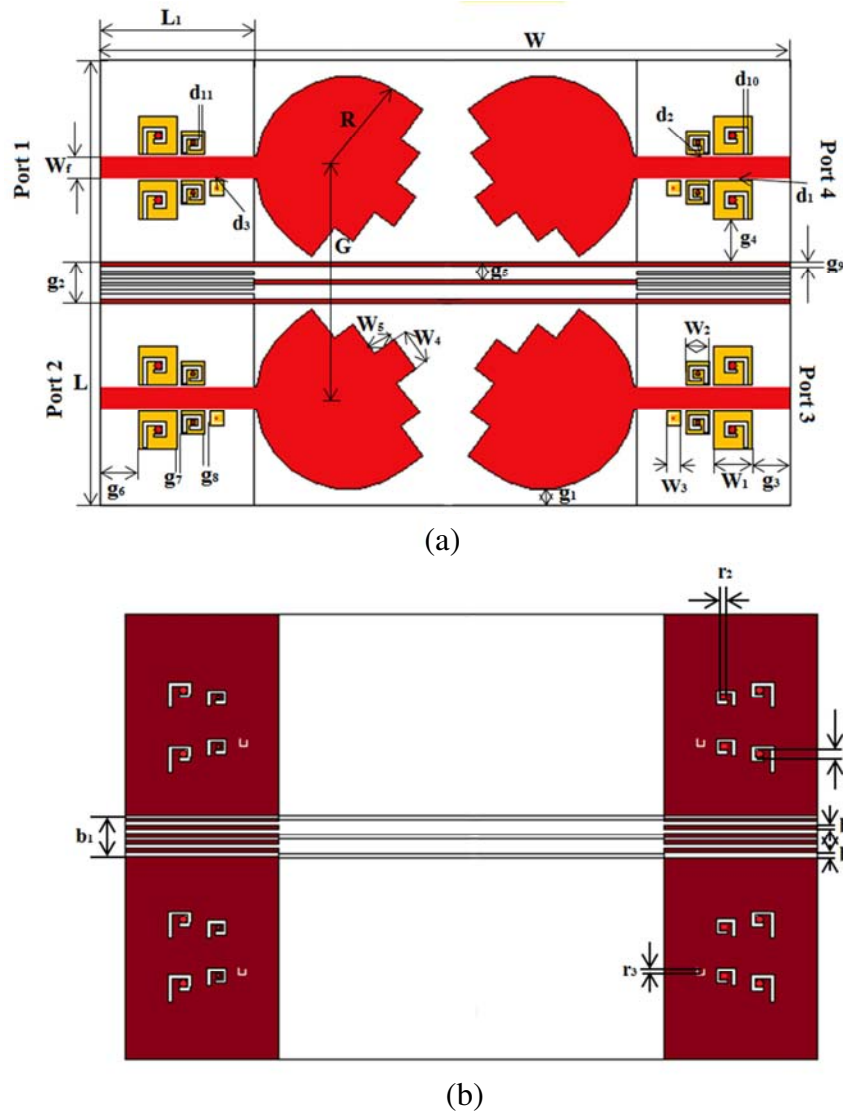


Figure 4. Design of proposed structure (a) top view, (b) backside view.

locations of notches in antenna 4 and antenna 5 remain identical. Fig. 9 shows simulated values of the mutual coupling among different antenna elements.

It can be seen that the magnitude of transmission coefficients among ports of proposed antenna is more than 15 dB throughout the UWB frequency range and hence qualifies for a MIMO antenna. When port 1 of the proposed antenna is excited, the current from port 1 tends to couple to port 2 but is blocked by the decoupling arrangement among the ports. It is verified through simulation and experimental results that the proposed antenna provides wide-band electromagnetic isolation over the operating frequency range. Fig. 10 shows the simulated and measured results of VSWR of the proposed antenna. It can be seen that WiMAX band is centered around 3.4 GHz with simulated and measured VSWR values of 5.2 and 4.7, respectively. WLAN band notch is centered around 5.5 GHz having simulated and measured VSWRs of 6.1 and 5.6, respectively. Similarly, X-band is centered around 7.6 GHz with simulated and measured values of 5.1 and 4.6, respectively. It can be seen throughout the paper that simulated and measured results show good resemblance. Minor variations can be seen in measured results due to fabrication and measurement errors. Fig. 11 shows the measured values of transmission coefficients. It can be seen that like simulated values of transmission coefficients, the measured magnitudes are also less than 15 dB.

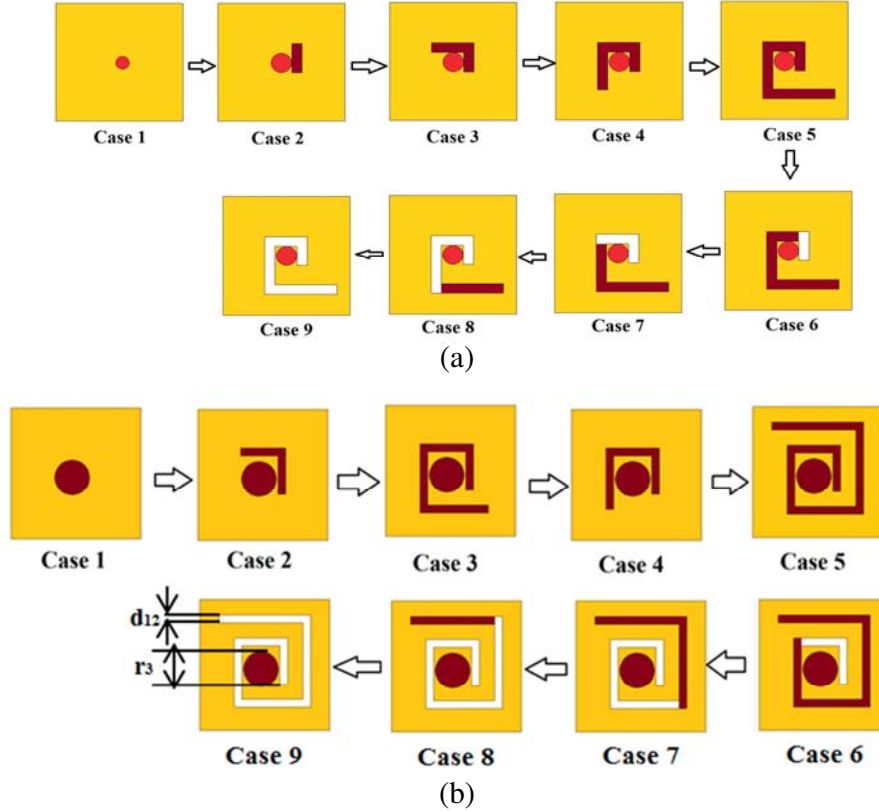


Figure 5. (a) Top view of IB-CEBG cells in WiMAX and WLAN bands, (b) top view of IB-CEBG cell in X-band.

Figure 12 shows the effect on VSWR when inductance is boosted using spiral shaped slots, and only WiMAX IB-CEBG structure is placed near the microstrip feed line. Case 9 gives the highest value of inductance and therefore the lowest value of resonant frequency. In Fig. 13, the same manner as the inductance enhancement effect is shown when one WLAN IB-CEBG cell is placed near the microstrip feedline. The inductance value is boosted as one moves from case 1 to case 9. Case 9 therefore gives the minimum value of resonant frequency. Fig. 14 shows the inductance enhancement effect when one X-band IB-CEBG is placed near the microstrip feed. The maximum inductance is associated with case 9, and hence minimum resonant frequency is obtained as per Equation (4).

The variation of change in the patch size of IB-CEBG structures on VSWR is given in Fig. 15, Fig. 16, and Fig. 17 for WiMAX, WLAN, and X-band notches, respectively. It must be easily observed from Equations (2) and (4) that by increasing the widths W_1 , W_2 , and W_3 , the value of capacitance increases, thereby decreasing the value of resonant frequency.

Figure 18 shows the variation in VSWR by varying the distance d_1 among the WiMAX IB-CEBG cells and microstrip feed. Fig. 19 shows the effect on VSWR when d_2 , i.e., separation among the microstrip feed and WLAN IB-CEBG cells, is varied. Similarly, Fig. 20 shows the variation in VSWR when distance d_3 among microstrip feed and X-band IB-CEBG structures varies. It can be concluded that if the spacing among the IB-CEBG cells and feedline decreases the magnitude of notch decreases. Similarly, if the spacing among the feed and IB-CEBG structures increases the magnitude on notch improves.

Each IB-CEBG structure is responsible for a band notch in its own band; however, minor fluctuations in other bands are also seen. This is because of electromagnetic coupling among different IB-CEBG structures. Fig. 21 gives the effect on VSWR when radii of vias for WiMAX and WLAN IB-CEBG structures are varied.

Via radius variation effect on VSWR can be verified from Equation (1) to Equation (4). It can

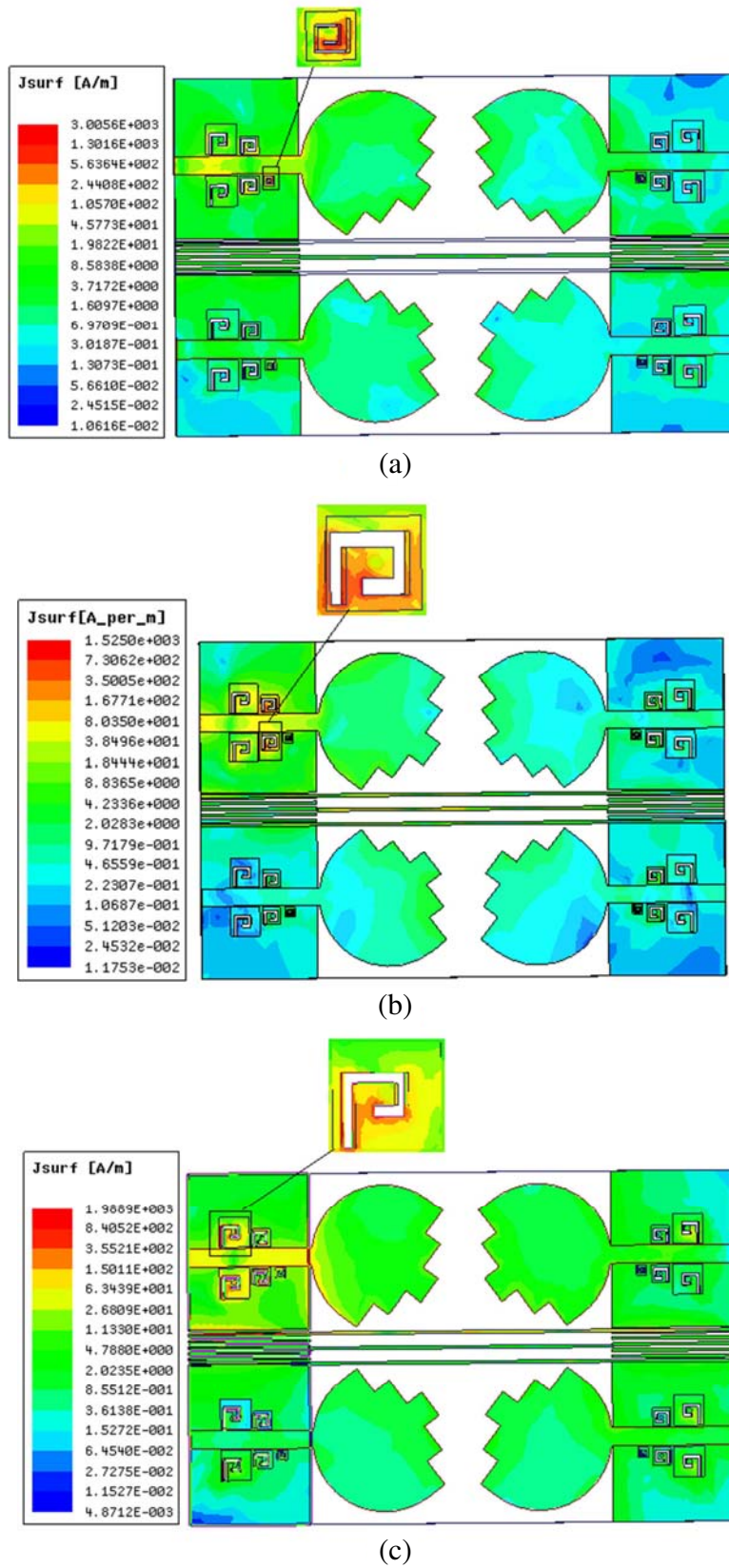


Figure 6. Current distribution on the proposed antenna at (a) 7.5 GHz, (b) 5.5 GHz, (c) 3.5 GHz.

Table 1. Measurements of the proposed antenna.

Specifications of the proposed antenna	Value (mm)
Antenna substrate width (W)	90
Ground plane size of proposed design (L_1)	20
Microstrip feed width (W_f)	3
Length of antenna Substrate (L)	58
Circular disc monopole radius (R)	12
Via radius for WiMAX IB-CEBG structures (r_1)	0.5
Stepped height on semi-circular monopole (W_5)	3.07
Via radius for WLAN IB-CEBG structures (r_2)	0.3
Decoupling structure strip width (d_1)	0.5
Via radius for 7.2–8.4 GHz band IB-CEBG (r_3)	0.25
Spacing among antenna feed and WiMAX IB-CEBG (g_2)	0.2
Space among WiMAX IB-CEBG and WLAN IB-CEBG (g_7)	0.52
Space between WLAN IB-CEBG & 7.2–8.4 GHz IB-CEBG (g_8)	0.78
Separation amid two antenna elements (G)	30
Separation linking feed line and X-band IB-CEBG (g_4)	0.25
Stepped width on semi-circular monopole (W_4)	4.8
Width of Slotted ground plane (b_1)	0.5
Separation on the side of elements (g_1)	2
Separation between decoupling elements (g_2)	2.5
Separation between feed line and WLAN IB-CEBG (g_3)	0.25
Separation between decoupling elements (g_5)	5.5
Separation among WiMAX IB-CEBG and decoupling element (g_4)	0.75
Stepped width on semi-circular monopole (W_4)	4.8
Edge length of IB-CEBG for 3.3–3.6 GHz band notch (W_1)	5
Slot width on WLAN IB-CEBG structure (d_{11})	0.5
Width of slot on X-band IB-CEBG structure (d_{12})	0.1
Separation between WiMAX IB-CEBG and antenna feed (g_2)	5
Edge length of IB-CEBG for 5–6 GHz band notch (W_3)	3
Patch width for IB-CEBG for X-band notch (W_2)	1.7
Ground plane slot width (b_3)	5.5
Separation between slots in ground plane (b_2)	0.5
Distance between Port 2 and WiMAX IB-CEBG cell (g_6)	5
Distance between Port 3 and WiMAX IB-CEBG cell (g_3)	5
Slot width on WiMAX IB-CEBG structure (d_{10})	0.5

be seen from Equation (1) that as the via radius (r) decreases, the inductance of structure is enhanced thus causing a shift in the resonant frequency (f_r) towards the lower frequencies using Equation (4). The proposed antenna gain can be improved by means of high impedance surface [54, 55] working as a reflector. This type of reflectors helps in back lobes minimisation and improvement in front to back ratio. As proposed in [56], IB-CEBG structures can also make antenna work in WiMAX and WLAN bands. In Fig. 22, it can be seen that the radiation efficiency of antenna is almost equal to 80%. The simulated and measured radiation characteristics are included in Fig. 23. Both co-polar and cross-polar radiation characteristics in E -plane and H -plane are shown. Similarly, Fig. 24 shows the simulated and

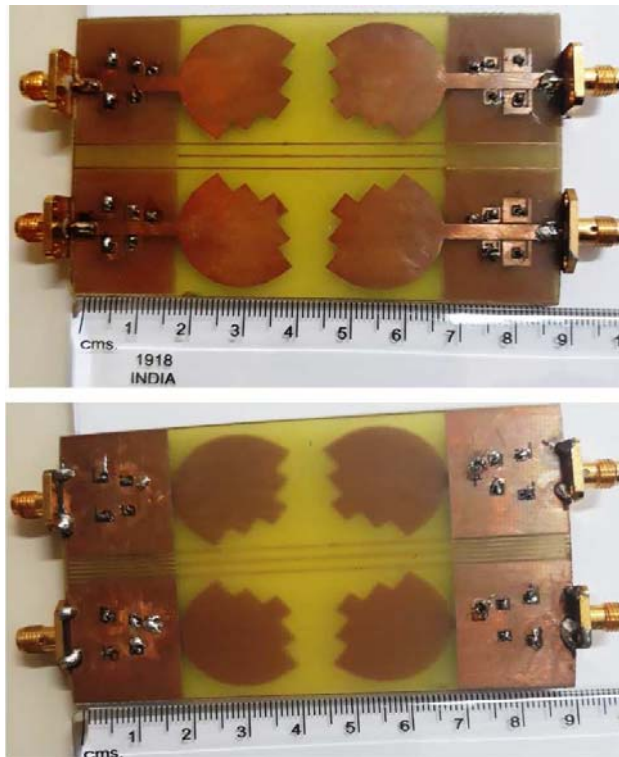


Figure 7. Front and backside view of the fabricated antenna.

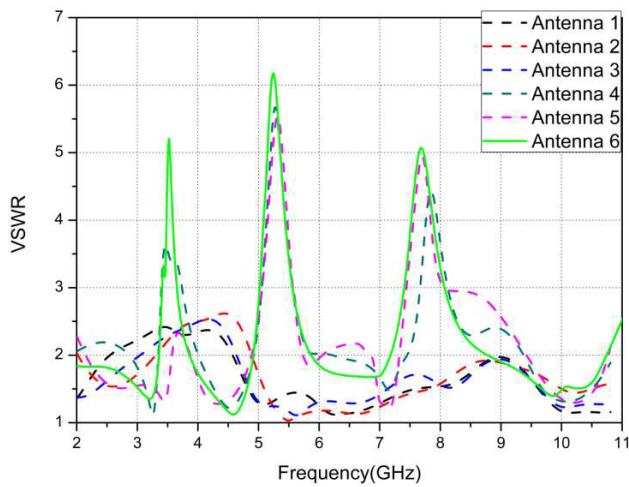


Figure 8. Comparison of proposed structure with five different antenna structures on the basis of VSWR variation.

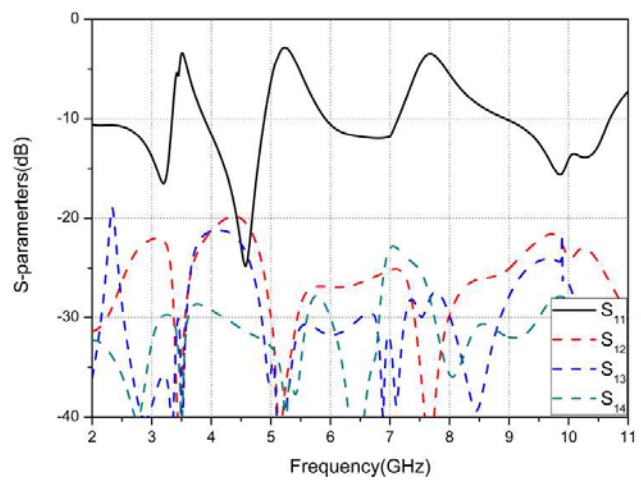


Figure 9. Effect of mutual coupling in different antenna ports of proposed antenna (simulated).

measured radiation characteristics at 10 GHz. Co-polar and cross-polar radiation patterns can be seen for both E -plane and H -plane.

To validate the simulated results, the measurement of antenna is carried out. In the measurement of radiation pattern, a horn antenna is used, which is placed at a suitable distance from the proposed antenna. The ECC (ρ_{ij}) is calculated using a far-field radiation pattern [57, 58] using the following

equation:

$$\rho_{ij} = \frac{\int_0^{2\pi} \int_0^\pi A_{ij}(\theta, \varphi) \sin \theta d\theta d\varphi}{\sqrt{\int_0^{2\pi} \int_0^\pi A_{ij}(\theta, \varphi) \sin \theta d\theta d\varphi \int_0^{2\pi} \int_0^\pi A_{jj}(\theta, \varphi) \sin \theta d\theta d\varphi}} \quad (5)$$

$$A_{ij}(\theta, \varphi) = E_{\theta,i}(\theta, \varphi)E_{\theta,j}^*(\theta, \varphi) + E_{\varphi,i}(\theta, \varphi)E_{\varphi,j}^*(\theta, \varphi) \quad (6)$$

where $E_{\theta/\varphi,i/j}(\theta, \varphi)$ in Equation (6) is the θ (or ϕ) polarized far-field electrical field values of antenna i (or j) in a spherical coordinate system. Envelope Correlation Coefficient (ECC) is of high importance for the proper performance of MIMO antenna design. ECC value can be calculated using Equation (5).

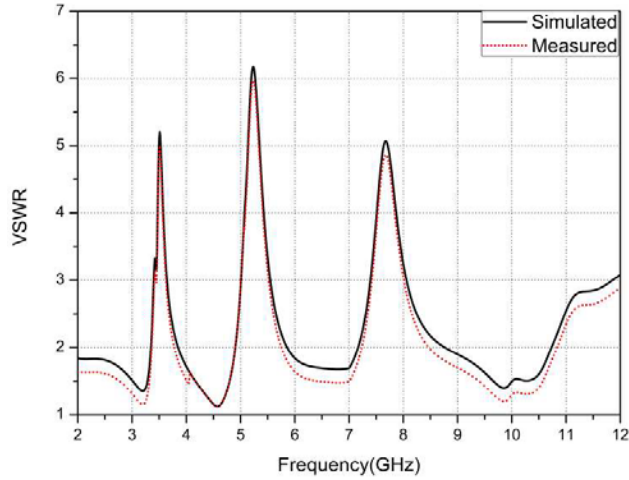


Figure 10. Plot of simulated and measured VSWR variation with frequency.

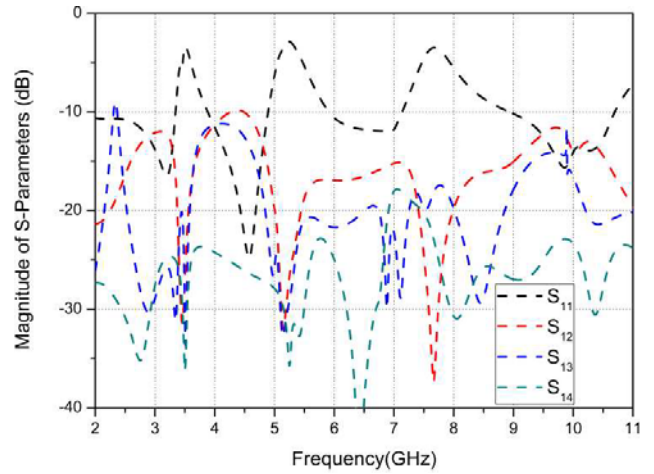


Figure 11. Measured results of variation of the mutual coupling with frequency of proposed antenna.

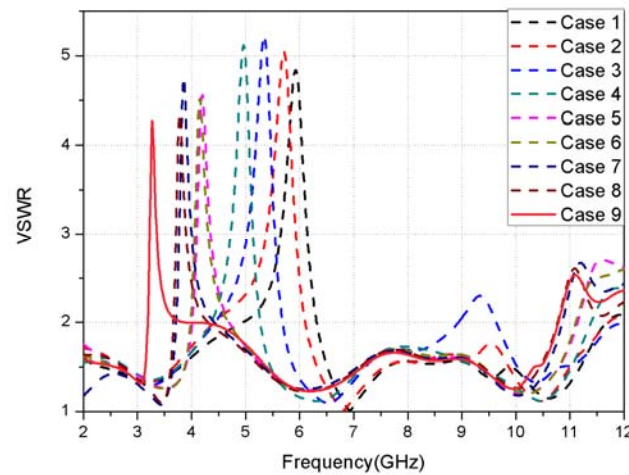


Figure 12. Effect on WiMAX notch frequencies when inductance is boosted for WiMAX IB-CEBG structure.

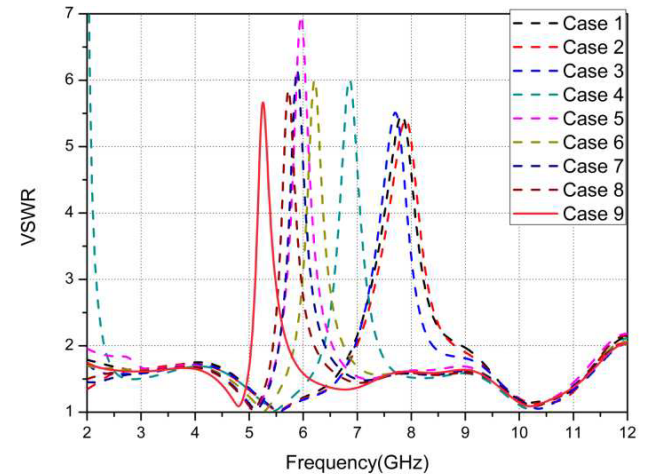


Figure 13. Effect on WLAN notch frequencies when inductance is boosted for WLAN IB-CEBG structure.

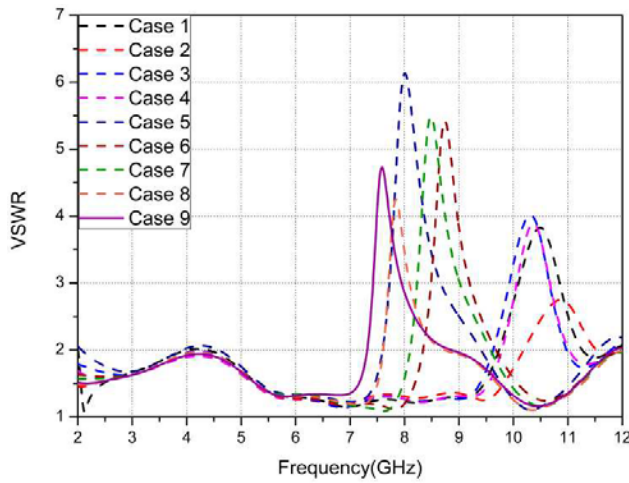


Figure 14. Effect on X-band notch frequency when inductance is boosted for X-band IB-CEBG structures.

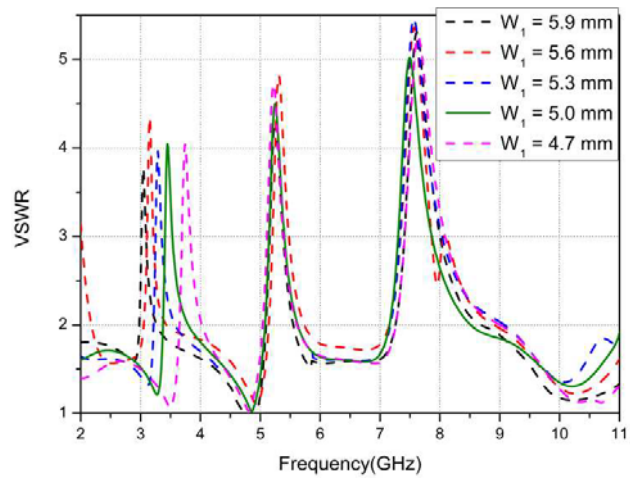


Figure 15. Effect on VSWR with variation in (W_1) of the proposed IB-CEBG structures.

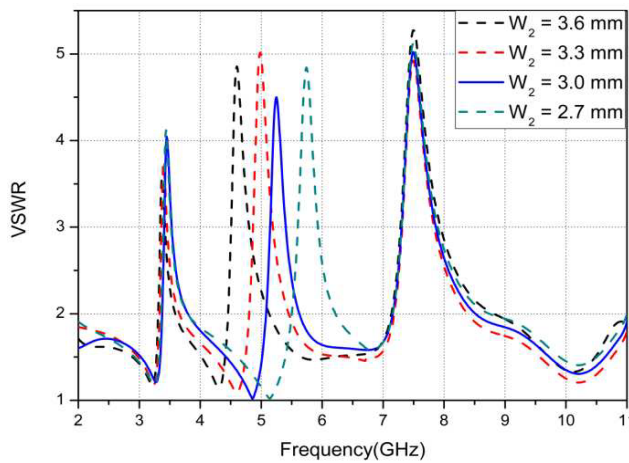


Figure 16. Effect on VSWR with variation in (W_1) of the proposed IB-CEBG structures.

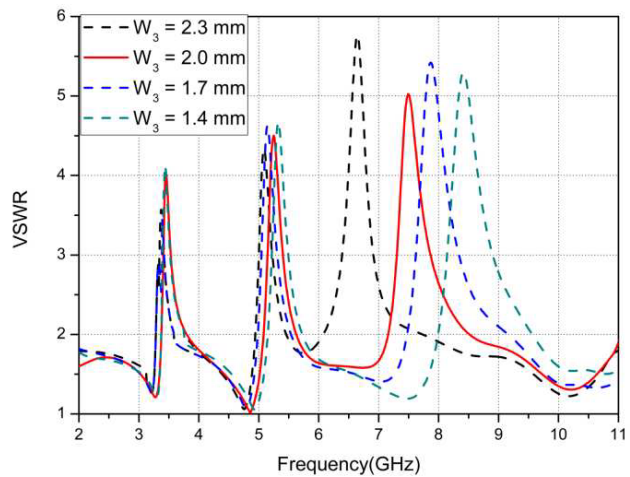


Figure 17. Effect on VSWR with variation in (W_1) of the proposed X-band IB-CEBG structures.

Fig. 25 illustrates simulated and measured ECC (ρ_{ij}) variations with frequency for the proposed notched UWB MIMO/diversity antenna. The ECC value for proposed antenna is calculated to be less than 0.5 through the UWB frequency range for the proposed antenna. Thus, the proposed antenna shows excellent diversity performance throughout the operating frequencies.

The proposed antenna therefore qualifies for excellent design that can be used in several wireless applications throughout the UWB frequency range. Comparison is shown in Table 2, and it can be concluded that the proposed IB-CEBG structures are quite compact compared with conventional mushroom EBG structures. IB-CEBG structures obtain size reductions of 45.9%, 50.0%, and 48.4% for WiMAX, WLAN, and X-bands, respectively. In Table 3, a comparison of the proposed antenna with different available techniques is shown. IB-CEBG structures can be designed at any frequency and can be used with almost every UWB antenna without disturbing the radiator and radiation pattern.

In Fig. 26, it is shown that antenna gain decreases to a negative value over the notched frequencies.

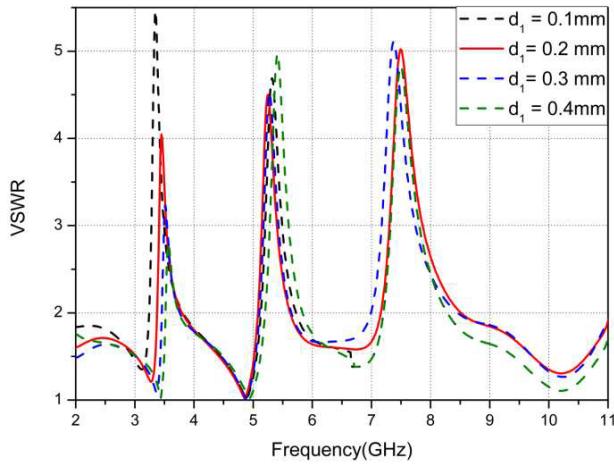


Figure 18. Variation in separation between microstrip line and WiMAX IB-CEBG cell.

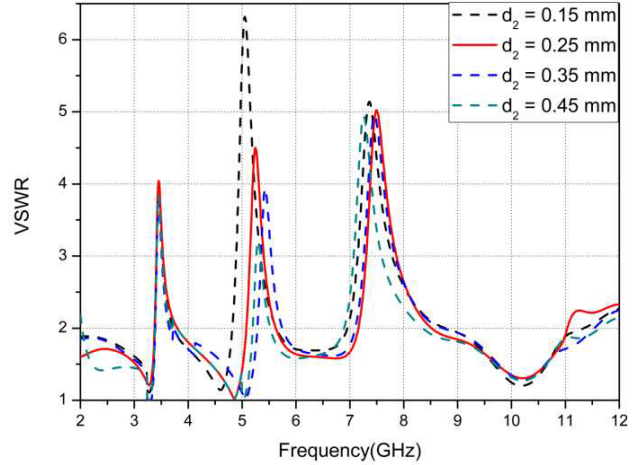


Figure 19. Effect of change in separation between microstrip line and WLAN IB-CEBG cell.

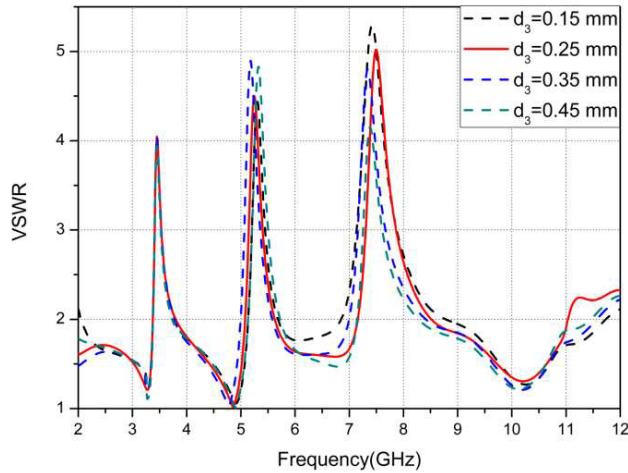


Figure 20. Effect of change in separation between microstrip line & WiMAX IB-CEBG cell.

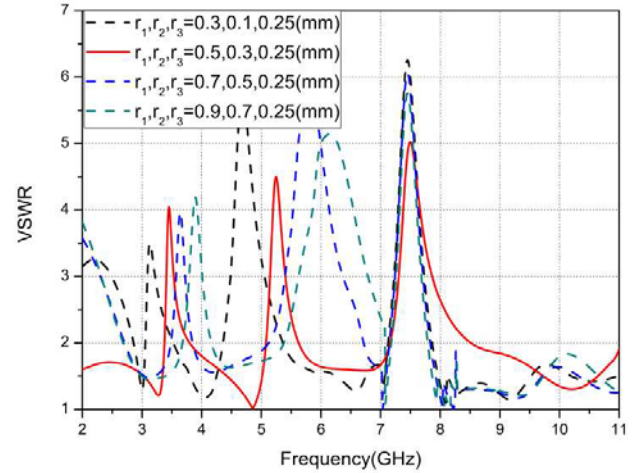


Figure 21. Via radiuseffect on notched frequencies of WiMAX and WLAN IB-CEBG cells.

Table 2. Comparisons among conventional and proposed IB-CEBG structures.

Band Notch	Conventional EBG structure	Proposed IB-CEBG structure	Percentage Compactness Achieved
WiMAX Band	9.25 mm	5 mm	45.9%
WLAN Band	6.1 mm	3 mm	50.0%
X-Band	3.3 mm	1.7 mm	48.5%

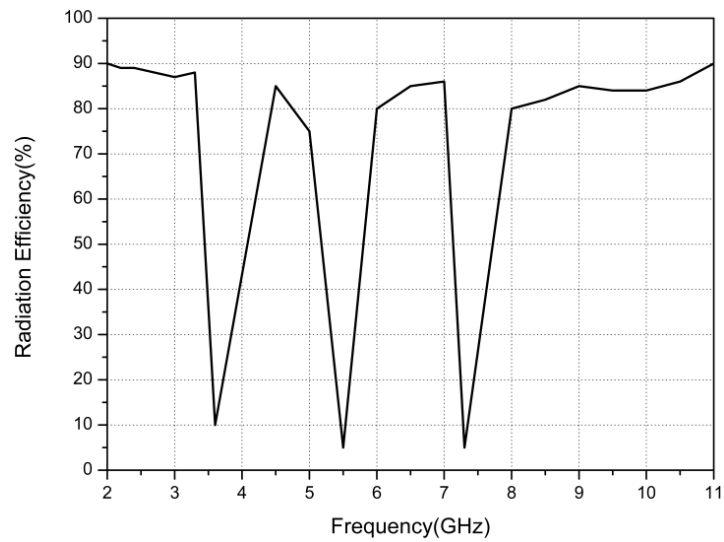


Figure 22. Radiation efficiency variation of proposed antenna.

Table 3. Comparisons of different notched frequency techniques available.

Ref.	Notch Techniques	Total number of radiators	Notched Frequency range (GHz)
[20]	Two EBG cells	1	4.98–5.43 & 5.64–5.93
[21]	Four EBG cells	1	5.15–5.95
[38]	Split ring resonators	2	WLAN Band
[59]	Trident shaped strips on microstrip line	2	5.4–5.86, 7.6–8.4
[60]	Radiator containing slit	4	5.15–5.925
[61]	L-type Stubs	2	3.62–4.77
[62]	Band stop design	4	5.15–5.825
[63]	EBG cells	4	WLAN Band
[64]	Spiral Shaped Slot	2	3.7–4, 5.75–6.05, 7.45–8.4
[65]	Strips in antenna ground	2	5.15–5.85
[66]	T-shaped Stub and CSRR	4	3.4–4.5
[67]	Pin diode and band stop design	4	5.15–5.825
[68]	CSRR	2	WLAN Band
[69]	Open stubs in radiator	2	WLAN Band
[70]	Pin diode and quarter wave stub	4	4.8–6.2
[71]	Novel Band stop design	4	WLAN Band
[72]	Parasitic stub, extended branch and rectangular slot	4	5–6
[73]	Mushroom EBG structures	4	WLAN Band
[74]	Crescent ring shaped resonator	4	4.0–5.2
[75]	Independent slits	2	WiMAX and WLAN
[76]	L-shaped slot, a T-shaped stub	2	3.87–5.94 GHz, 7.04–8.7 GHz
Proposed antenna	Five IB-CEBG cells	4	WLAN, WiMAX and X-band

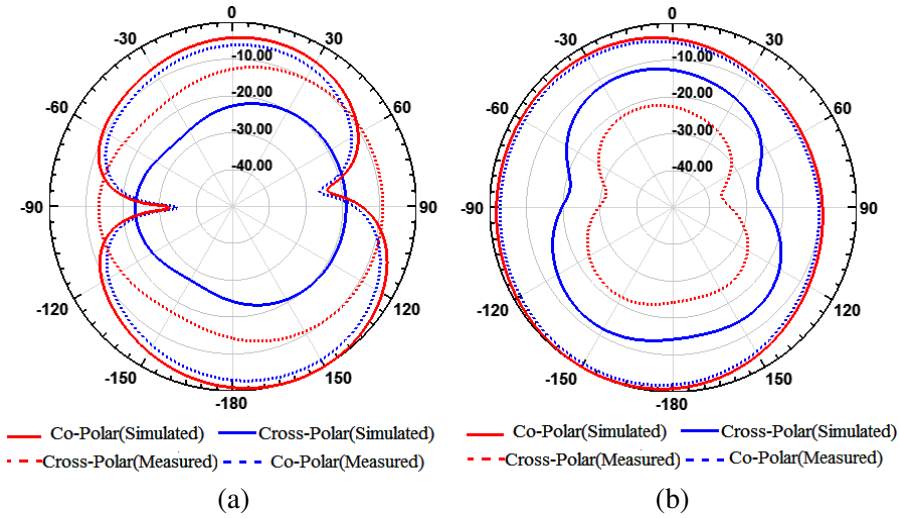


Figure 23. Plot of radiation field at 4.5 GHz in (a) *E*-plane and (b) *H*-plane.

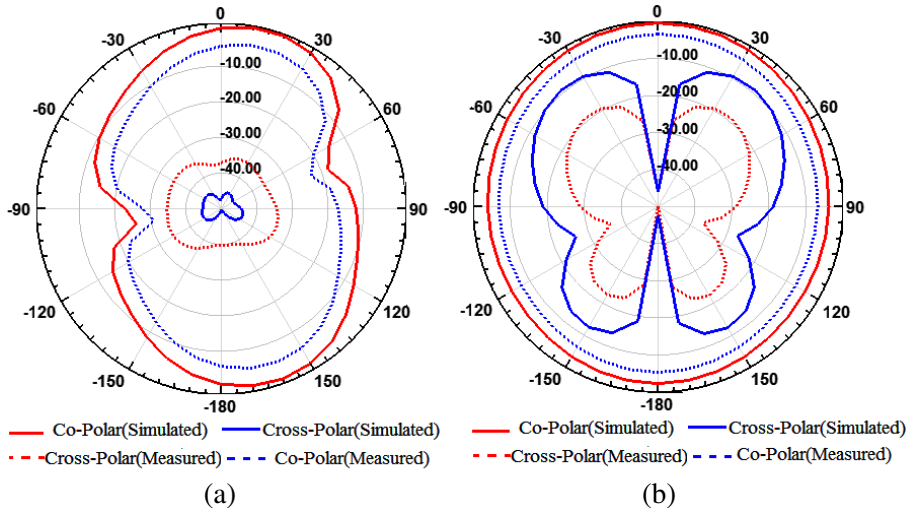


Figure 24. Plot of radiation field at 10 GHz in (a) *E*-plane and (b) *H*-plane.

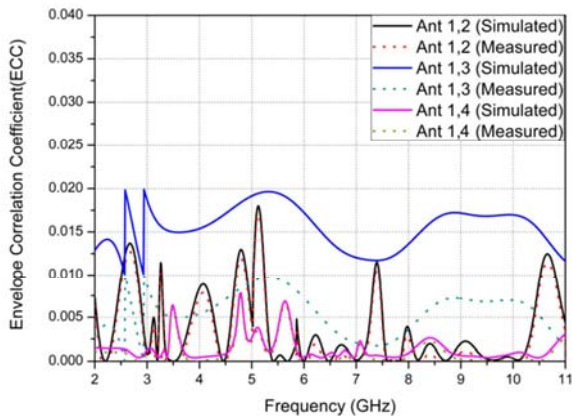


Figure 25. Variation of ECC with frequency among different antenna elements of proposed antenna.

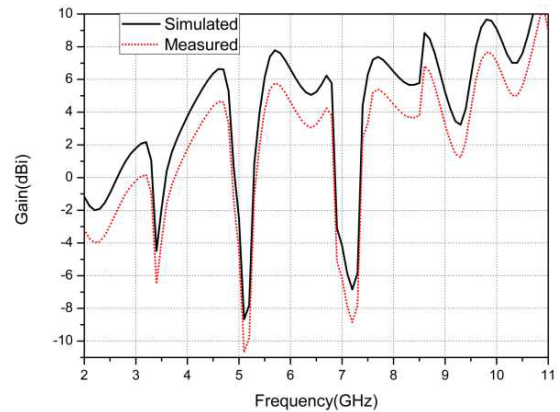


Figure 26. Antenna gain variation with frequency.

5. CONCLUSION

A triple band notched UWB MIMO/Diversity antenna with IB-CEBG structures is elaborated in this research. IB-CEBG structures are used to obtain notches at interfering frequencies. The antenna rejects narrowband interfering sources, which works in WiMAX band (3.3–3.6 GHz), WLAN band (5–6 GHz), and X-band (7.2–8.4 GHz). A low cost FR-4 substrate is used in the fabrication of the proposed antenna having overall dimensions of $58 \times 90 \times 1.6 \text{ mm}^3$. The simulated and measured values of mutual coupling among antenna elements are found less than 15 dB. The value of ECC is less than 0.5 over the complete UWB frequency range which makes the proposed design an excellent choice for diversity applications. The simulated and measured values are in good resemblance. The proposed antenna can work as an excellent design for various wireless communication applications.

REFERENCES

1. Federal Communications Commission, "Revision of Part 15 of the Commission's rules regarding ultra-wideband transmission systems," Tech. Rep. ET-Docket 98-153, FCC02-48, Federal Communications Commission (FCC), Washington, DC, USA, 2002.
2. Liang, J., C. C. Chiau, X. Chen, and C. G. Parini, "Printed circular disc monopole antenna for ultra-wideband applications," *Electron. Lett.*, Vol. 40, No. 20, 1246–1248, 2004.
3. Sarkar, D., K. Sarkar, and K. Saurav, "A compact microstrip-fed triple band-notched UWB monopole antenna," *IEEE Antennas Wireless Propag. Lett.*, Vol. 13, 396–399, 2014.
4. Foudazi, A., H. R. Hassani, and S. M. Ali Nezhad, "Small UWB planar monopole antenna with added GPS/GSM/WLAN bands," *IEEE Trans. Antennas Propag.*, Vol. 60, No. 6, 2987–2992, 2012.
5. Li, W. T., X. W. Shi, and Y. Q. Hei, "Novel planar UWB monopole antenna with triple band-notched characteristics," *IEEE Antennas Wireless Propag. Lett.*, Vol. 8, 1094–1098, 2009.
6. Nguyen, D. T., D. H. Lee, and H. C. Park, "Very compact printed triple band-notched UWB antenna with quarter-wavelength slots," *IEEE Antennas Wireless Propag. Lett.*, Vol. 11, 411–414, 2012.
7. Zhu, F., S. Gao, A. T. S. Ho, A. Al Hameed, et al., "Multiple band-notched UWB antenna with band-rejected elements integrated in the feed line," *IEEE Trans. Antennas Propag.*, Vol. 61, No. 5, 3952–3960, 2013.
8. Trang, N. D., D. H. Lee, and H. C. Park, "Design and analysis of compact printed triple band-notched UWB antenna," *IEEE Antennas Wireless Propag. Lett.*, Vol. 10, 403–406, 2011.
9. Tang, M. C., S. Xiao, T. Deng, D. Wang, et al., "Compact UWB antenna with multiple band-notches for WiMAX and WLAN," *IEEE Trans. Antennas Propag.*, Vol. 59, 1372–1376, 2011.
10. Almalkawi, M. and V. Devabhaktuni, "Ultrawideband antenna with triple band-notched characteristics using closed-loop ring resonators," *IEEE Antennas Wireless Propag. Lett.*, Vol. 10, 959–962, 2011.
11. Mohammadian, N., M. N. Azarmanesh, and S. Soltani, "Compact ultra-wideband slot antenna fed by coplanar waveguide and microstrip line with triple-band-notched frequency function," *IET Microw. Antennas Propag.*, Vol. 4, 1811–1817, 2010.
12. Deng, J. Y., Y. Z. Yin, S. G. Zhou, and Q. Z. Liu, "Compact ultra-wideband antenna with tri-band notched characteristics," *Electron. Lett.*, Vol. 44, No. 21, 1231–123, 2008.
13. Vendik, I. B., A. Rusakov, K. Kanjanasit, J. Hong, et al., "Ultrawideband (UWB) planar antenna with single-dual- and triple-band notched characteristic based on ring resonator," *IEEE Antennas Wireless Propag. Lett.*, Vol. 16, 1597–1600, 2017.
14. Liu, Y., Z. Chen, and S. Gong, "Triple band-notched aperture UWB antenna using hollow-cross-loop resonator," *Electron. Lett.*, Vol. 50, 728–730, 2014.
15. Cai, Y. Z., H. C. Yang, and L. Y. Cai, "Wideband monopole antenna with three band-notched characteristics," *IEEE Antennas Wireless Propag. Lett.*, Vol. 13, 607–610, 2014.

16. Mohammed, H. J., et al., "Design of a uniplanar printed triple band-rejected ultra-wideband antenna using particle swarm optimisation and the fire-fly algorithm," *IET Microw. Antennas Propag.*, Vol. 10, 31–37, 2016.
17. Ali, W. A. E. and R. M. A. Moniem, "Frequency reconfigurable triple band-notched ultra-wideband antenna with compact size," *Progress In Electromagnetics Research C*, Vol. 73, 37–46, 2017.
18. Wang, Q. and Y. Zhang, "Design of a compact UWB antenna with triple band-notched characteristics," *Int. J. Antennas Propag.*, Vol. 892765, 1–9, 2014.
19. Abdelhalim, C. and D. Farid, "A compact planar UWB antenna with triple controllable band notched characteristics," *Int. J. Antennas Propag.*, Vol. 848062, 1–10, 2014.
20. Peng, L. and C. Ruan, "UWB band-notched monopole antenna design using electromagnetic-bandgap structures," *IEEE Trans. on Microwave Theory and Techniques*, Vol. 59, 1074–1081, 2011.
21. Yazdi, M. and N. Komjani, "Design of a band-notched UWB monopole antenna by means of an EBG structure," *IEEE Trans. on Antennas and Wireless Propagation*, Vol. 10, 170–173, 2011.
22. Jensen, M. A. and J. W. Wallace, "A review of antennas and propagation for MIMO wireless communication," *IEEE Trans. Antennas Propag.*, Vol. 52, 2810–2824, 2004.
23. Song, Y., N. Guo, and R. C. Qiu, "Implementation of UWB MIMO time-reversal radio testbed," *IEEE Antennas Wireless Propag. Lett.*, Vol. 10, 796–799, 2011.
24. Ben, I. M., L. Talbi, M. Nedil, and K. Hettak, "MIMO-UWB channel characterization within an underground mine gallery," *IEEE Trans. Antennas Propag.*, Vol. 60, 4866–4874, 2012.
25. Song, Y., T. N. Guo, R. C. Qiu, and M. C. Wicks, "A real time UWB MIMO system with programmable transmit waveforms: Architecture, algorithms and demonstrations," *IEEE Trans. Antennas Propag.*, Vol. 60, No. 8, 3933–3940, 2012.
26. Fletcher, P. N., M. Dean, and A. R. Nix, "Mutual coupling in multi element array antennas and its influence on MIMO channel capacity," *Electron. Lett.*, Vol. 39, No. 2, 342–344, 2003.
27. Lu, S., T. Hui, and M. Bialkowski, "Optimizing MIMO channel capacities under the influence of antenna mutual coupling," *IEEE Antennas Wireless Propag. Lett.*, Vol. 7, 287–290, 2008.
28. Chiu, C.-Y., C.-H. Cheng, R. D. Murch, and C. R. Rowell, "Reduction of mutual coupling between closely packed antenna elements," *IEEE Trans. Antennas Propag.*, Vol. 55, No. 4, 1732–1738, 2007.
29. Kokkinos, T., E. Liakou, and A. P. Feresidis, "Decoupling antenna elements of PIFA arrays on handheld devices," *IET Electron. Lett.*, Vol. 44, No. 25, 1442–1444, 2008.
30. Karaboikis, M., C. Soras, G. Tsachtsiris, and V. Makios, "Compact dual-printed inverted-F antenna diversity systems for portable wireless devices," *IEEE Antennas Wireless Propag. Lett.*, Vol. 3, No. 1, 9–14, 2004.
31. Chiau, C. C., X. Chen, and C. G. Parini, "A miniature dielectric-loaded folded half-loop antenna and ground plane effects," *IEEE Antennas Wireless Propag. Lett.*, Vol. 4, No. 1, 459–462, 2005.
32. Gao, Y., X. Chen, Z. Ying, and C. Parini, "Design and performance investigation of a dual-element PIFA array at 2.5 GHz for MIMO terminal," *IEEE Trans. Antennas Propag.*, Vol. 55, No. 12, 3433–3441, 2007.
33. Yang, F. and Y. Rahmat-Samii, "Microstrip antennas integrated with electromagnetic band-gap (EBG) structures: A low mutual coupling design for array applications," *IEEE Trans. Antennas Propag.*, Vol. 51, No. 10, 2936–2946, 2003.
34. Rajo-Iglesias, E., O. Quevedo-Teruel, and L. Inclan-Sanchez, "Mutual coupling reduction in patch antenna arrays by using a planar EBG structure and a multilayer dielectric substrate," *IEEE Trans. Antennas Propag.*, Vol. 56, No. 4, 1648–1655, 2008.
35. See, T. S. P. and Z. N. Chen, "An ultra wideband diversity antenna," *IEEE Trans. Antennas Propag.*, Vol. 57, No. 4, 1597–1605, 2009.
36. Rajagopalan, A., G. Gupta, A. S. Konanur, B. Hughes, et al., "Increasing channel capacity of an ultrawideband MIMO system using vector antennas," *IEEE Trans. Antennas Propag.*, Vol. 55, No. 10, 2880–2887, 2007.

37. Zhang, S., B. K. Lau, A. Sunesson, and S. He, "Closely-packed UWB MIMO/diversity antenna with different patterns and polarizations for USB dongle applications," *IEEE Trans. Antennas Propag.*, Vol. 60, No. 9, 4372–4380, 2012.
38. Gao, P., S. He, X. Wei, Z. Xu, et al., "Compact printed UWB diversity slot antenna with 5.5-GHz band-notched characteristics," *IEEE Antennas Wireless Propag. Lett.*, Vol. 13, 376–379, 2014.
39. Yoon, H. K., Y. J. Yoon, H. Kim, and C. H. Lee, "Flexible ultra-wideband polarization diversity antenna with band-notch function," *IET Microw. Antennas Propag.*, Vol. 5, No. 12, 1463–1470, 2011.
40. Lee, J. M., K. B. Kim, H. K. Ryu, and J. M. Woo, "A compact ultrawideband MIMO antenna with WLAN band-rejected operation for mobile devices," *IEEE Antennas Wireless Propag. Lett.*, Vol. 11, 990–993, 2012.
41. Li, J. F., Q. X. Chu, Z. H. Li, and X. X. Xia, "Compact dual band-notched UWB MIMO antenna with high isolation," *IEEE Trans. Antennas Propag.*, Vol. 61, No. 9, 4759–4766, 2013.
42. Chacko, B. P., G. Augustin, and T. A. Denidni, "Uniplanar polarization diversity antenna for wideband systems," *IET Microw. Antennas Propag.*, Vol. 7, No. 10, 851–857, 2013.
43. Liu, L., S. W. Cheung, and T. I. Yuk, "Compact MIMO antenna for portable UWB applications with band-notched characteristic," *IEEE Trans. Antennas Propag.*, Vol. 63, No. 3, 1917–1924, 2015.
44. Li, J.-F., D.-L. Wu, and Y.-J. Wu, "Dual band-notched UWB MIMO antenna with uniform rejection performance," *Progress In Electromagnetics Research M*, Vol. 54, 103–111, 2017.
45. Toktas, A., "G-shaped band-notched ultra-wideband MIMO antenna system for mobile terminals," *IET Microw. Antennas Propag.*, Vol. 11, No. 3, 718–725, 2017.
46. Yang, F. and Y. Rahmat-Samii, *Electromagnetic Band Gap Structures in Antenna Engineering*, Cambridge University Press, 2009.
47. Jaglan, N., S. D. Gupta, B. K. Kanaujia, and S. Srivastava, "Band notched UWB circular monopole antenna with inductance enhanced modified mushroom EBG structure," *Wireless Networks*, Vol. 24, No. 2, 383–393, 2016.
48. Sievenpiper, D., "High-impedance electromagnetic surfaces," Ph.D. dissertation, Department of Electrical Engineering, University of California, Los Angeles, CA, 1999.
49. Sohn, J. R., K. Y. Kim, H.-S. Tae, and H. J. Lee, "Comparative study on various artificial magnetic conductors for low-profile antenna," *Progress In Electromagnetics Research*, Vol. 61, 27–37, 2006.
50. Jaglan, N., S. D. Gupta, B. K. Kanaujia, S. Srivastava, and E. Thakur, "Triple band notched DG-CEBG structures based UWB MIMO/diversity antenna," *Progress In Electromagnetics Research C*, Vol. 80, 21–37, 2018.
51. Jaglan, N., S. D. Gupta, B. K. Kanaujia, and S. Srivastava, "Design and development of an efficient EBG structures based band notched UWB circular monopole antenna," *Wireless Personal Communication*, Vol. 96, No. 2, 5757–5783, Springer, 2017.
52. Ahmed, O. and A. R. Sebak, "A printed monopole antenna with two steps and a circular slot for UWB applications," *IEEE Antennas Wireless Propag. Lett.*, Vol. 7, 411–413, 2008.
53. Naghar, A., et al., "Design of compact wideband multi-band and ultrawideband band pass filters based on coupled half wave resonators with reduced coupling gap," *IET Microw. Antennas Propag.*, Vol. 9, No. 15, 1786–1792, 2015, doi: 10.1049/iet-map.2015.0188.
54. Saraswat, R. K. and M. Kumar, "A frequency band reconfigurable UWB antenna for high gain applications," *Progress In Electromagnetics Research B*, Vol. 64, 29–45, 2015.
55. Mu, X., W. Jiang, S.-X. Gong, and F.-W. Wang, "Dual-band low profile directional antenna with high impedance surface reflector," *Progress In Electromagnetics Research Letters*, Vol. 25, 67–75, 2011.
56. Saraswat, R. K. and M. Kumar, "Miniaturized slotted ground UWB antenna loaded with metamaterial for WLAN and WiMAX applications," *Progress In Electromagnetics Research B*, Vol. 65, 65–80, 2016.
57. Diallo, A., P. L. Thuc, C. Luxey, R. Staraj, G. Kossiavas, M. Franzén, and P. S. Kildal, "Diversity characterization of optimized two-antenna systems for UMTS handsets," *EURASIP Journal on*

- Wireless Communication and Networking*, Hindawi Publishing Corporation, 2007.
58. Srivastava, G. and A. Mohan, "Compact MIMO slot antenna for UWB applications," *IEEE Antennas Wireless Propag. Lett.*, Vol. 15, 1057–1060, 2015.
 59. Jetti, C. R. and V. R. Nandanavanam, "Trident shape strip loaded dual band notched UWB MIMO antenna for portable device applications," *AEU-International Journal of Electronics and Communications*, Vol. 83, 11–21, 2018.
 60. Zhu, J., S. Li, B. Feng, L. Deng, et al., "Compact dual polarized UWB quasi-self-complementary MIMO/diversity antenna with band rejection capability," *IEEE Antennas Wireless Propag. Lett.*, Vol. 15, 905–908, 2016.
 61. Chandel, R. and A. K. Gautam, "Compact MIMO/diversity slot antenna for UWB applications with band-notched characteristics," *Electron. Lett.*, Vol. 52, 336–338, 2016.
 62. Khan, M. S., A. D. Capobianco, S. Asif, A. Iftikhar, et al., "Compact 4×4 UWB-MIMO antenna with WLAN band rejected operation," *IET Electronic Letters*, Vol. 51, No. 14, 1048–1050, 2015.
 63. Kiem, N. K., H. N. B. Phuong, and D. N. Chien, "Design of compact 4×4 UWB MIMO antenna with WLAN band rejection," *Int. J. Antennas Propag.*, Vol. 539094, 1–11, 2014.
 64. Irene, G. and A. Rajesh, "A Penta-band reject inside cut koch fractal hexagonal monopole UWB MIMO antenna for portable devices," *Progress In Electromagnetics Research C*, Vol. 82, 225–235, 2018.
 65. Kang, L. and H. Li, "Compact offset microstrip-fed MIMO antenna for band-notched UWB application," *IEEE Antennas Wireless Propag. Lett.*, Vol. 14, 1754–1757, 2015.
 66. Kumar, S., R. Kumar, R. K. Vishwakarma, and K. Srivastava, "An improved compact MIMO antenna for wireless applications with band-notched characteristics," *International Journal of Electronics and Communications*, Vol. 90, 20–29, 2018.
 67. Khan, M. S., A. Iftikhar, S. Asif, A.-D. Capobianco, et al., "A compact four elements UWB MIMO antenna with on-demand WLAN rejection," *Microwave and Optical Technology Letters*, Vol. 58, No. 2, 270–276, 2016.
 68. Yadav, D., M. P. Abegaonkar, S. K. Koul, V. N. Tiwari, and D. Bhatnagar, "Two element band-notched UWB MIMO antenna with high and uniform isolation," *Progress In Electromagnetics Research M*, Vol. 63, 119–129, 2018.
 69. Kang, L., H. Li, X.-H. Wang, and X.-W. Shi, "Miniaturized band notched UWB MIMO antenna with high isolation," *Microwave and Optical Technology Letters*, Vol. 58, No. 2, 878–881, 2016.
 70. Khan, M. S., A. Naqvi, B. Ijaz, M. F. Shafique, et al., "Compact planar UWB MIMO antenna with on-demand WLAN rejection," *IET Electronic Letters*, Vol. 51, No. 13, 963–964, 2015.
 71. Khan, M. S., A. D. Capobianco, S. Asif, A. Iftikhar, et al., "Compact 4×4 UWB-MIMO antenna with WLAN band rejected operation," *Electron. Lett.*, Vol. 51, No. 14, 1048–1050, 2015.
 72. Tao, J. and Q. Feng, "Compact UWB band-notch MIMO antenna with embedded antenna element for improved band notch filtering," *Progress In Electromagnetics Research C*, Vol. 67, 117–125, 2016.
 73. Kiem, N. K., H. N. B. Phuong, and D. N. Chein, "Design of compact 4×4 UWB-MIMO antenna with WLAN band rejection," *Int. J. Antennas Propag.*, 1–11, 2014.
 74. Wu, W., B. Yuan, and A. Wu, "A quad-element UWB MIMO antenna with band-notch and reduced mutual coupling based on EBG structures," *Int. J. Antennas Propag.*, 1–10, 2018.
 75. Raheja, D. K., S. Kumar, and B. K. Kanaujia, "Compact quasi-elliptical-self-complementary four-port super-wideband MIMO antenna with dual band elimination characteristics," *AEU-International Journal of Electronics and Communications*, Vol. 114, 153001, 2020, doi: 10.1016/j.aeue.2019.153001.
 76. Srivastava, K., A. Kumar, B. K. Kanaujia, and S. Kumar, "A CPW-fed UWB MIMO antenna with integrated GSM band and dual band notches," *Int. J. RF Microw. Comput.-Aided Eng.*, Vol. 29, No. 1, 21433, 2019, doi: 10.1002/mmce.21433.